Solid Freeform Fabrication 2017: Proceedings of the 28th Annual International Solid Freeform Fabrication Symposium – An Additive Manufacturing Conference
Reviewed Paper

TECHNOLOGICAL CHALLENGES FOR AUTOMOTIVE SERIES PRODUCTION IN LASER BEAM MELTING

Felix Haeckel M.Sc.*, Dipl. Ing. Maximilian Meixlsperger*, Dipl. Ing. Torsten Burkert*

*BMW Group, Additive Manufacturing Center, Hufelandstraße 5, 80788 Munich, Germany

Abstract

Compared to traditional production methods, Additive Manufacturing enables a tool free production leading to higher flexibility, freedom of design and lightweight potential. For these reasons the BMW Group is proceeding from the production of prototypes to the direct series production of parts.
For metal components, the process of selective Laser Beam Melting is able to realize these potentials. Aside from the economic issues, technological challenges also have to be met. Among them is achieving consistent part quality in the production of same parts. To achieve technical specifications compliant in series production, a defined process stability and reproducibility of the part properties is needed.
This reproducibility is investigated for the process of selective Laser Beam Melting. Also variables which have the biggest impact on the part quality throughout a simulated series production are being examined. Thus the reproducibility of the process can be quantified. To guarantee a high and stable part quality in the future, approaches are being developed to monitor or systematically prevent influences, which are found to have a negative effect on the process quality.

Introduction

During the past few years, the trend of digitalization came to the forefront of production engineering. In this context new production techniques have been evolving and gradually improving over time. Among them, the Additive Manufacturing Technologies gained importance for having the ability to manufacture physical parts, tool-free, directly out of digital data [1]. Due to the increasing productivity, the evolution from technologies for producing prototype-parts to a series technology has begun to take place [2–4].
In medical engineering and aerospace, Additive Manufacturing (AM) is already established as a production technique for parts, which are installed in the final products [4]. In the automotive industry, the lot size and pressure on costs is higher compared to the previously named industrial sectors. This presents a challenge to produce high volume parts with AM in a series process. Nevertheless, small series productions have already been put into practice [5,6]. The consistent development of the processes induces a large increase in productivity and thereby lower costs. Due to this benefit, it can be assumed, that in the future more series components will be manufactured by Additive Manufacturing Technologies.
In the sector of metal additive manufacturing, the process of selective Laser Beam Melting has great potential. Besides the productivity, the reproducibility of the process has to be granted within automotive series production. To meet these requirements, it is necessary to analyze the state of the art of the reproducibility and offer possibilities to optimize and monitor the process.

Methodology

The reproducibility of the selective Laser Beam Melting process will be investigated with respect to the part quality and under the assumption of series production of equivalent parts.
The quality in terms of the mechanical properties of a laser melted part is among others, dependent on the porosity of the part, as described in *Brandl, 2011* [7], Wycisk, 2014 [8] or *Gong, 2015* [9]. To analyze the reproducibility of the porosity level, a series production of a defined and specifically designed specimen will be simulated. As it can be seen in figure 1, the specimen begins with a cuboid with an edge length of 10 mm and maximum height of 14 mm, when the support structure is taken into account. Above the cuboid a cylinder with a length of 82 mm and a diameter of 14.1 mm will be manufactured. Above this cylinder, an additional cuboid is placed, so that the total specimen measures a height of 106 mm. Both cuboids serve to analyze the part porosity level via an incident light microscope and further digital image evaluation. The porosity level will be furthermore named as relative part density and can be calculated using formula (1).

(1) *Rel. part density in % = 100 % - area of porosity in %*

The investigations will be performed on two machines with a specific material for each machine (cf. figure 1). By comparison, one machine, the SLM Solutions SLM 500 HL, labeled below as Machine 1 with the aluminum alloy AlSi10Mg has rather large build chamber. The second machine is a ReaLizer SLM 100, labeled below as machine 2, with the tool steel X3NiCoMoTi18-9-5 (material number 1.2709). By means of this methodology, general process characteristics shall be identified instead of machine or material dependent ones. The materials were chosen because they are standard materials for additive manufacturing in the automotive industry.

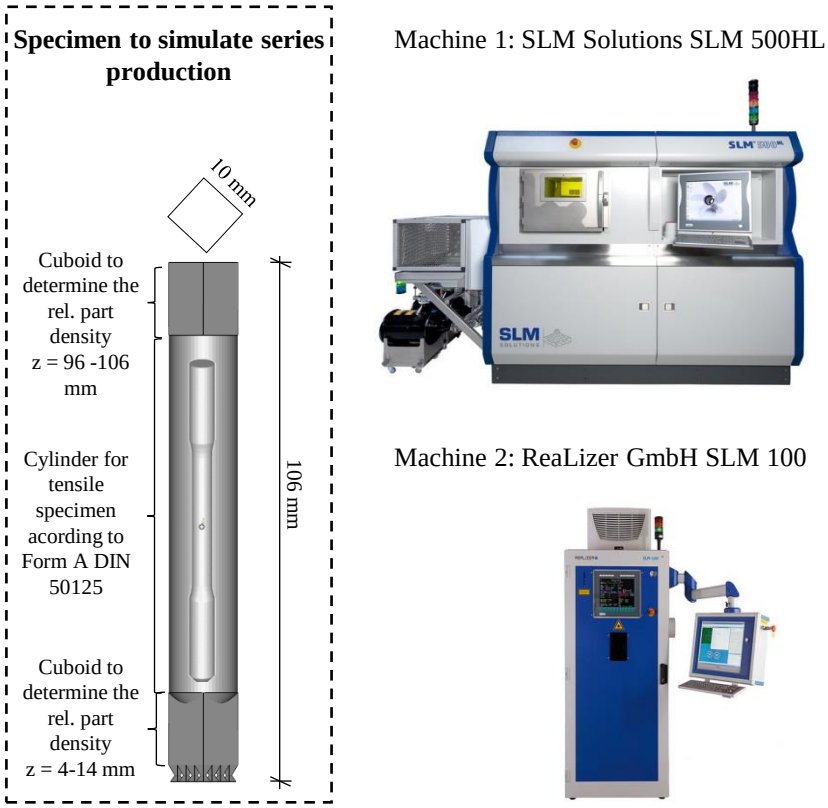

Figure 1 Used specimens and machines for simulating a series production of equivalent parts

Upfront to the investigations, stable machine and scan parameters are being identified and will be applied on every build job. Also the procedure of the machine preparation and the laser scanning strategy are identical for each build job. The only variation is the number of the manufactured specimens on each build platform. In the following, this will be referred to as the packing density. Which can be calculated using formula (2).

(2) Packing density in % = [Part volume / (base area max. height)] * 100*

The different packing densities are investigated on each machine, 5 % (13 % in case of machine 2), 25 % and 45 %. A packing density above 45 % could not be achieved with standard automotive parts. Therefore 45 % is the chosen upper limit. Each packing density will be manufactured six times and nine specimen will be analyzed after each build job. Those nine specimen (highlighted red in figure 2) are equally distributed over the build platform to investigate the homogeneity of the part quality over the build area. Thus, the part quality in terms of the porosity and mechanical properties can be investigated as a function of the machines packing density and the position in the build chamber. The blue highlighted parts are reservoirs to monitor the powder quality. These investigations are not part of this paper.
Figure 2 gives an overview of the build jobs and the labelling.

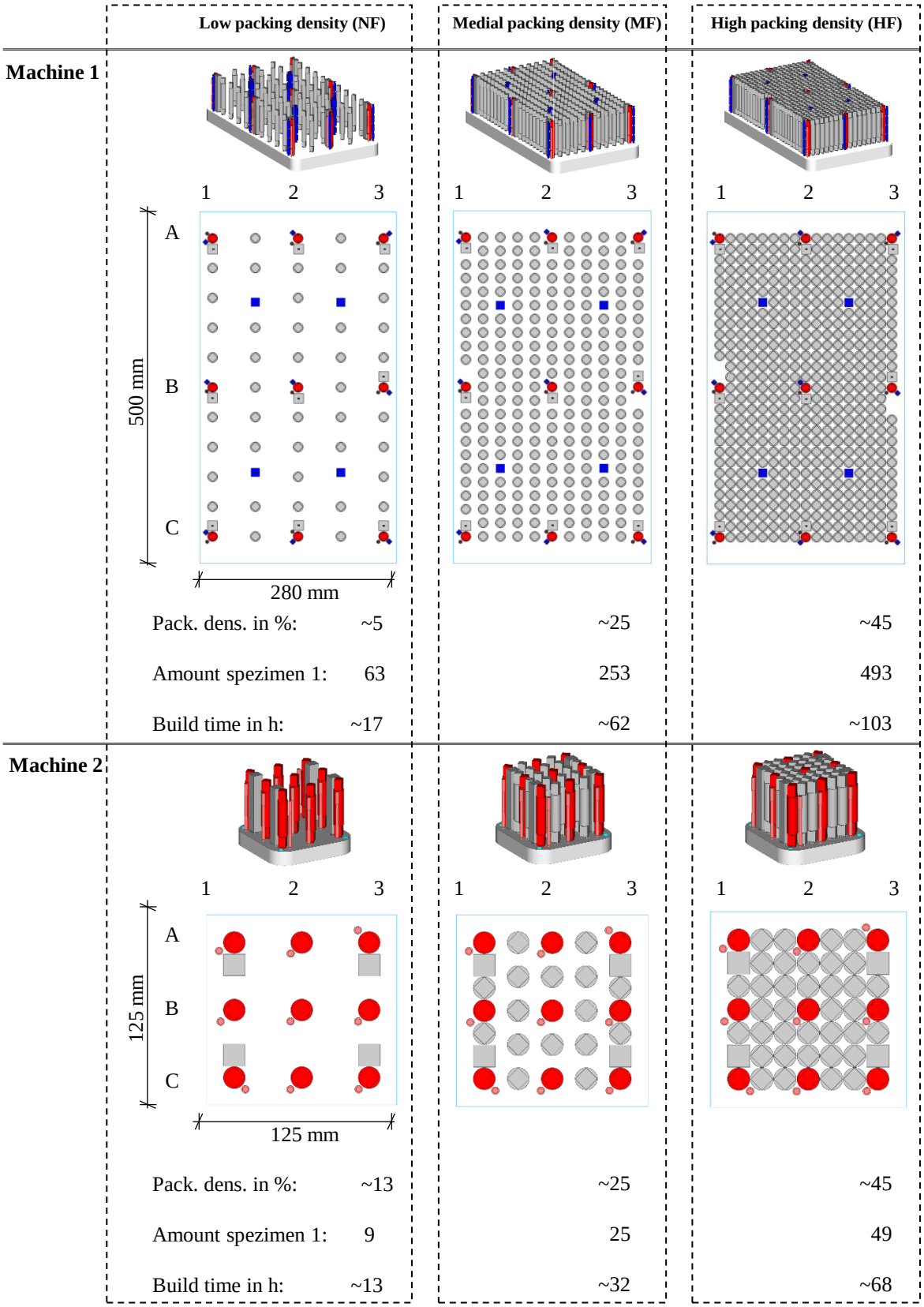

Figure 2 Overview of the build jobs to analyze the reproducibility and labelling

Results

In this chapter the results of the reproducibility analysis with respect to the relative part density and the mechanical properties will be presented. Figure 3 shows the relative part densities on machine 1 and the material AlSi10Mg. The relative part density is presented with regard to the maximum height, z = 110 mm and z = 10 mm, (cf. "rel. part density overview) and the distribution of the frequency of occurrence. On the x-axes in upper figure all manufactured build jobs are represented (NF cf. to the lowest packing density, Mf cf. to the middle packing density and HF to the highest packing density). Furthermore, the mean values and standard deviations, related to the packing density, are presented.

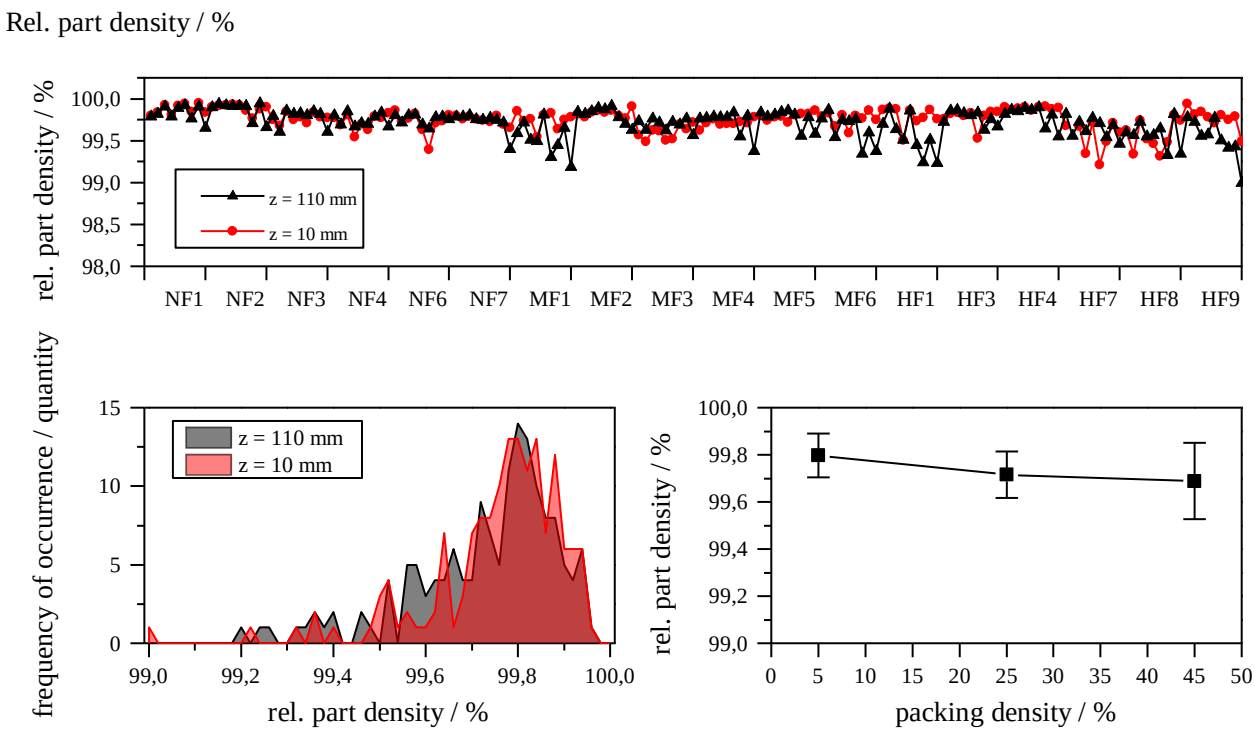

Figure 3 Results for the rel. part densities on Machine 1

Except a few outliers the relative part density is higher than 99 % for all parts. This value is characteristic of Aluminum-alloys fabricated with selective Laser Beam Melting (cf. [10,11]). It can be seen that increasing the packing density leads to both a decrease of the mean value and an increase of the standard deviation. Furthermore it can be seen, that the relative part density decreases over the build time, in other words the relative density for the cuboid positioned at the z-level of 110 mm is much lower than the part density for the cuboid at the z-level of 10 mm (black line, cf. build job numbers MF1, MF4 MF6, HF1, HF8, HF9). Only build job HF7 reveals an opposing effect.
The results of machine 2 with the material 1.2709 are presented in figure 4 and analogous to the results on machine 1.

Rel. part density

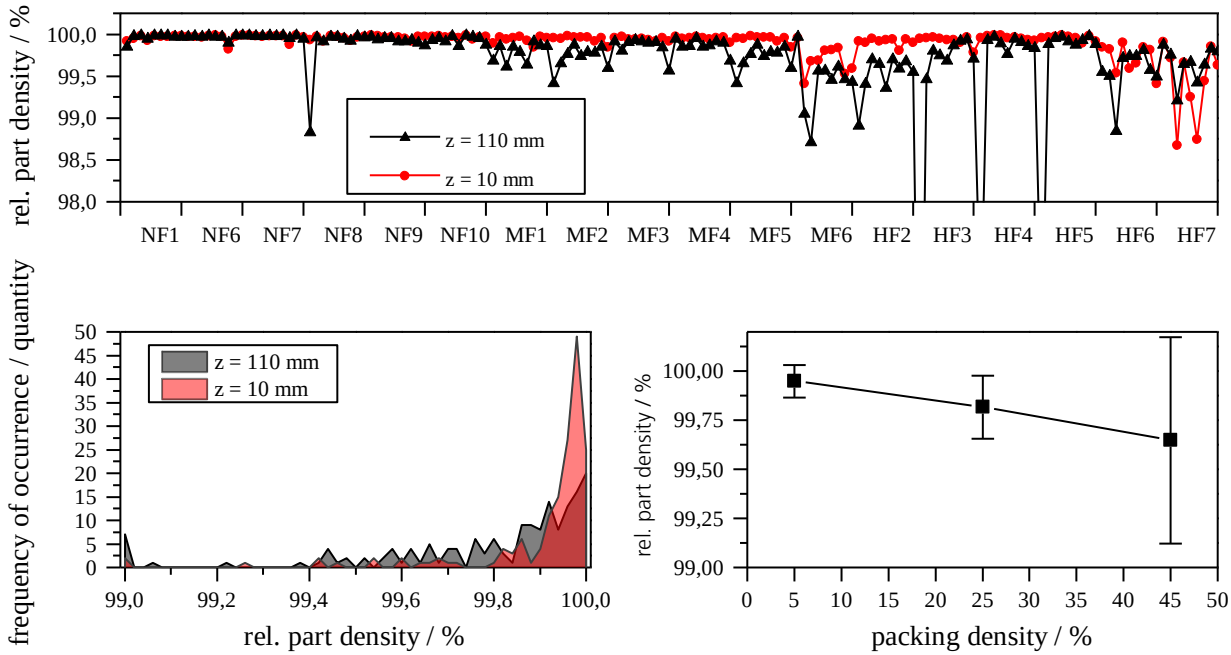

Figure 4 Results for the rel. part densities on Machine 2

The results for the relative part densities on machine 2 follow the same trends as on machine 1 but are more pronounced. The mean value decreases and the standard deviation increases in a more incisive way. The difference between the cuboid at a z-level of 10 mm and the one on 110 mm is more significant. Furthermore, more outliers with part densities below 99 % can be identified (one outlier appeared with a density of 93.9 %).

The mechanical properties follow the same trend as the relative part densities for both machines and materials. Figure 5 displays the tensile strength Rm, the yield strength Rp0.2 and the elongation at break, At, for machine 1 and AlSi10Mg. The analyzed specimen are investigated "as built" without any further heat treatment.

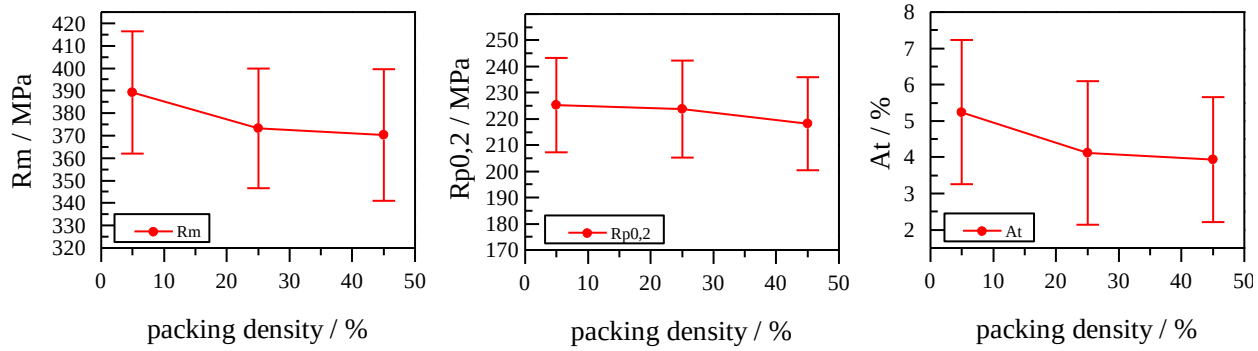

Figure 5 Quasi static mechanical properties for machine 1(AlSi10Mg), tensile strength Rm, yield strength Rp0.2, elongation at break At

It can be seen, that the mean value for each property decreases if the packing density rises. This phenomena is also recognizable for the mean values of the mechanical properties on machine 2 and the material 1.2709 (cf. figure 6).

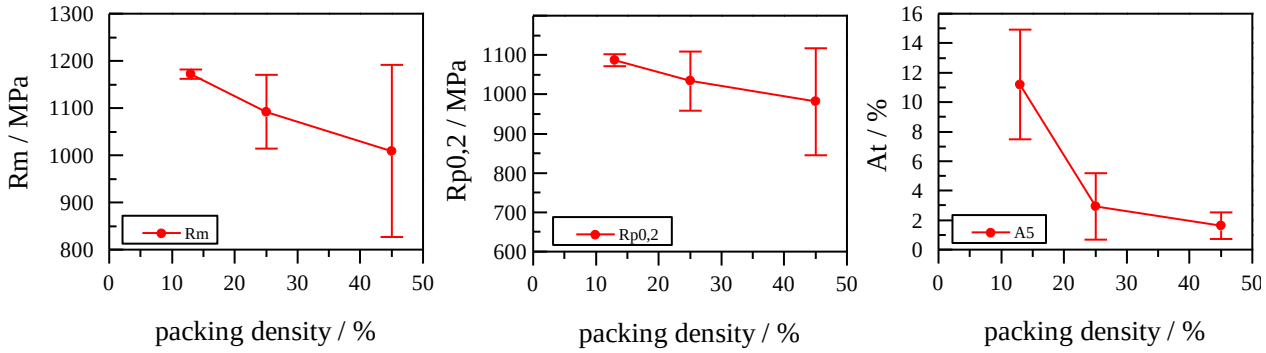

Figure 6 Quasi static mechanical properties for machine 2 (1.2709), tensile strength Rm, yield strength Rp0.2, elongation at break At

Beyond that, it can be seen, that for tensile and yield strength, the standard deviation increases if the packing density increases. The standard deviation of the elongation at break At decreases for increasing packing density because the mean value is already very low, leading to the fact that outliers beneath the mean value do not have much leverage.

The trends of the mechanical properties and the relative part densities reveal a clear correlation between the two factors. As described in the methodology, this correlation was already detected among others in *Brandl, 2011* [7] or *Gong, 2015* [8]. In the following, the relative part densities polished cross sections are being investigated via an incident light microscope.

Figure 7 shows “best case” and “worst case” images of cross sections.

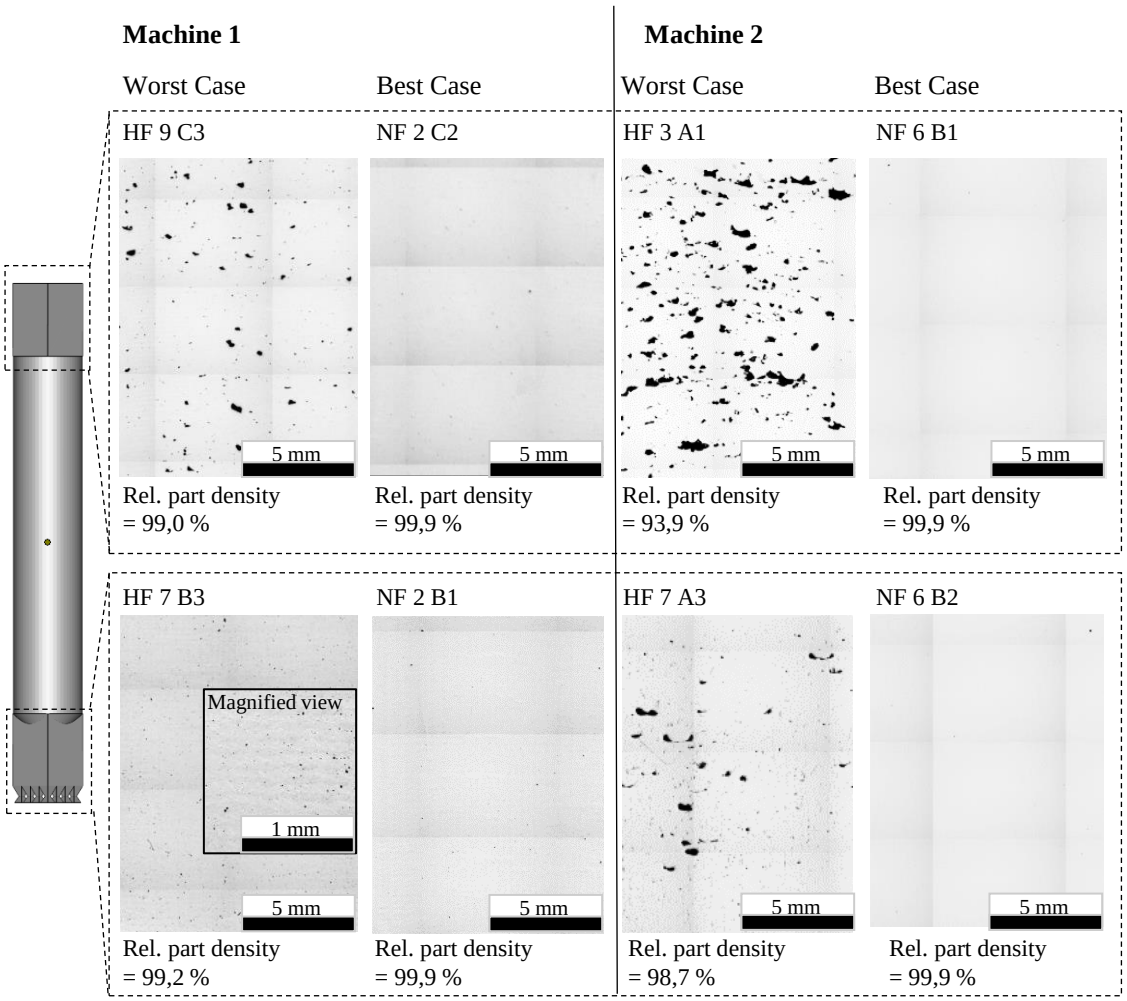

Figure 7 Polished cross sections to show "best case" and "worst case" parts according to the relative part densities and in dependence of the elevation level

It can be seen that mainly pores > 50 µm and a sharp form contribute to a higher porosity. One exception is the "worst case" on machine 2 and the part label HF8 B3. The porosity of 0.7 % is achieved by a multitude of fine pores below 50 µm. Further noticeable is that the "worst case" parts always appear within build jobs with the highest packing density (45 %). On the other hand, the "best case" parts originate from build jobs with the lowest packing density (5 and 13 %).

As it can be seen in the figures 3, 4 and 7, the porosity increases during the build jobs. The cuboids at a z-level of max. 110 mm are characterized by a higher porosity and also the amount of pores with bigger diameters than 50 µm increases. To clarify this phenomena the process by-products (PbP) has to be taken into account. Figure 8 provides an overview of important PbPs and variations of influencing factors.

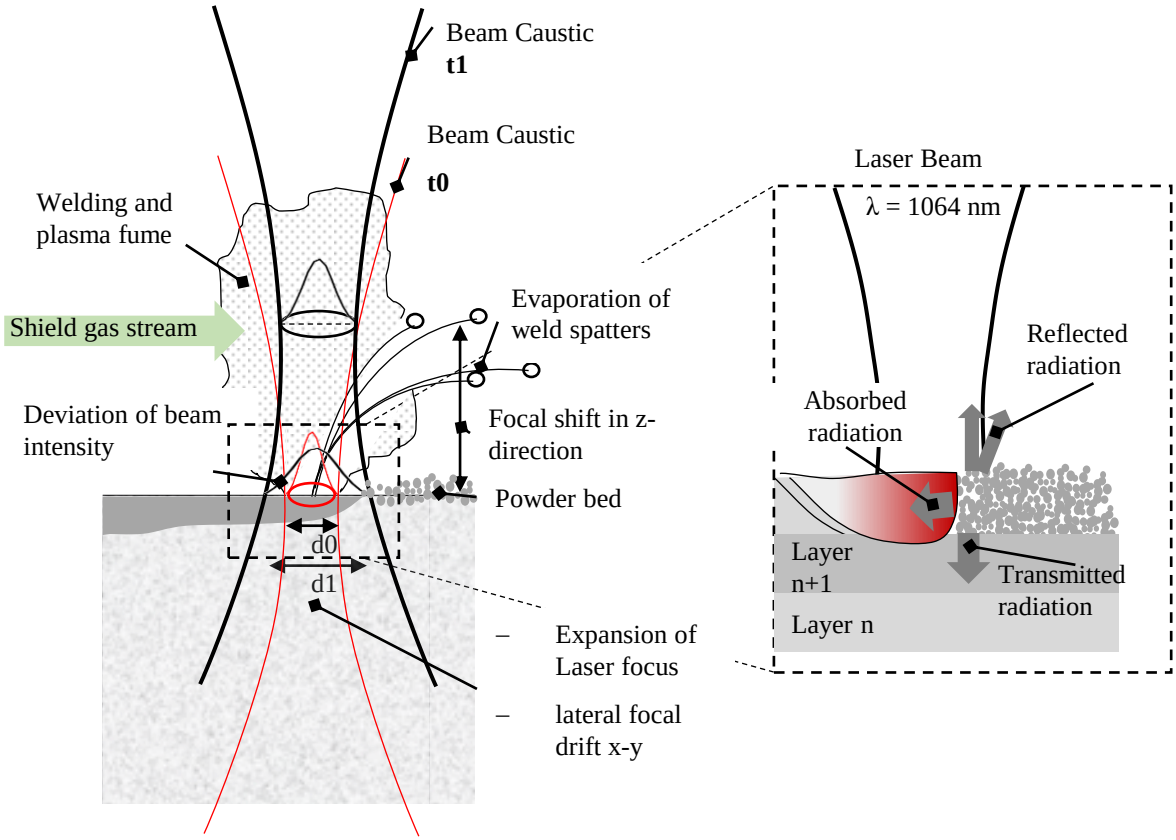

Figure 8 Process interactions end effects during a Laser Beam Melting process [12]

During the interaction of the energy of the Laser and the powder, weld fume arises and weld spatters get evaporated out of the melt pool. Among others, *Repossini et al*., 2016 [13], Liu, 2015 [14] investigated the weld spatter behavior of the selective Laser Beam Melting process as well as *Ladewig, 2016* [12],who analyzed the influence of the shield gas stream on process by-products. An explanation of the occurrence of weld spatters is given in [15]. Due to different thermal states of the optical system components during a build job, the position of the laser focus alters. This effect was investigated by *Kühnle et al*., *2012* [16]. This leads to different energy densities at the processing level.

To identify the cause of the formation of pores bigger than 50 µm, etched and polished cross sections are being analyzed. With this method, both the weld seams and foreign objects, which are welded in the microstructure and form pores bigger than 50 µm (cf. figure 9), are being revealed.

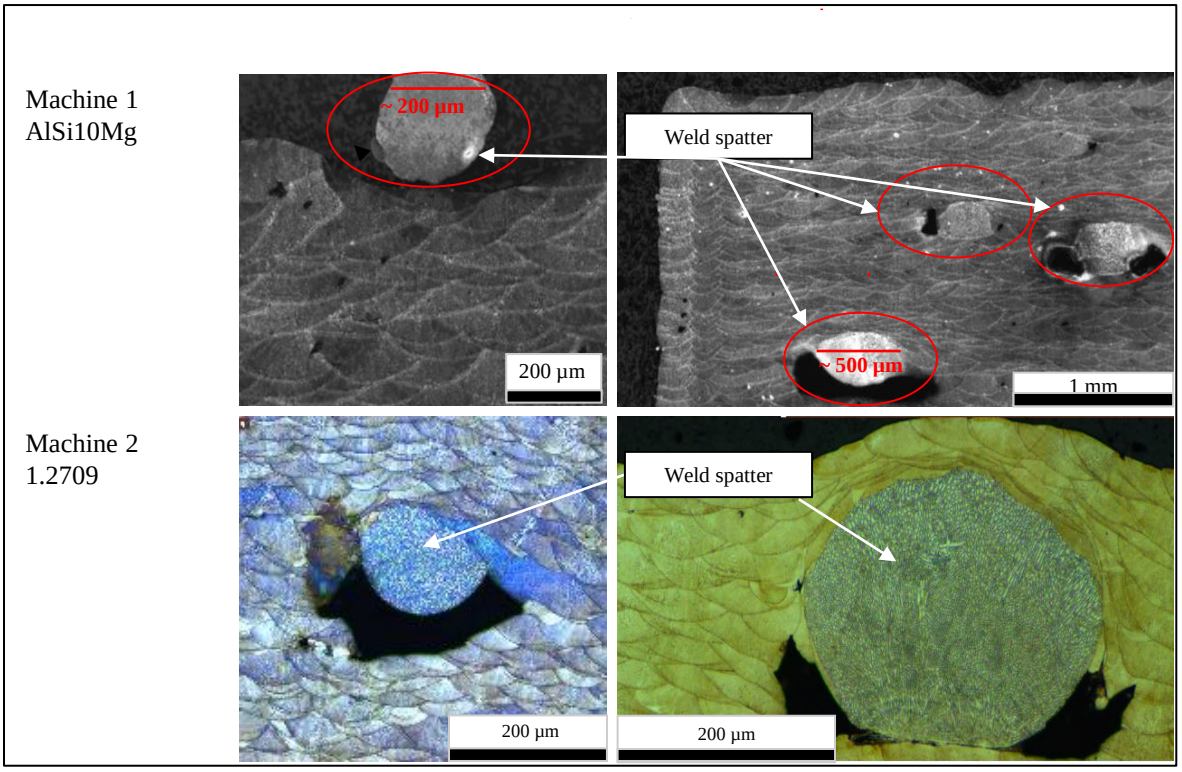

Figure 9 Polished and edged cross sections to identify the cause of porosity > 50 µm

Based on theirs size and form, the assumption is obvious that the visible particles are weld spatters, which evaporated out of the melt pool during the welding process. The existence of weld spatter porosity was already mentioned in [17,18,12]. Those particles characteristically have diameters between the size of 200 and 500 µm. Therefore they have a many times higher volume than the biggest powder particles, with a d90 value of 60 µm. The introduced energy of the laser radiation is not sufficient to entirely melt those particles. This leads to a shielding function for the laser radiation and the formation of the pores.

In order to analyze the phenomena that the amount of pores > 50 µm increases over the build time, a special investigation was set up. The factor varying over the build time is the cleanliness of the process chamber. The laser protection glass (PG) gets contaminated with weld fume and surplus powder gets dropped beside the recoating system. To examine the influence of those two factors, a build job with high packing density is produced. After the process, the build chamber and protection glass are left contaminated and another build job of high packing density is started, but only up to a height of 10 mm. After that build job, the first influencing factor is removed by cleaning the protection glass and a further additional build job is produced on top of the existing one. Subsequently, the next influencing factor, the contaminated process chamber, is removed by cleaning (also the PG was cleaned again) and the third build job is produced on top of the two existing jobs. Figure 10 gives an overview of the three build jobs and the state of the process time dependent influence factors, as well as the result in terms of the porosity.

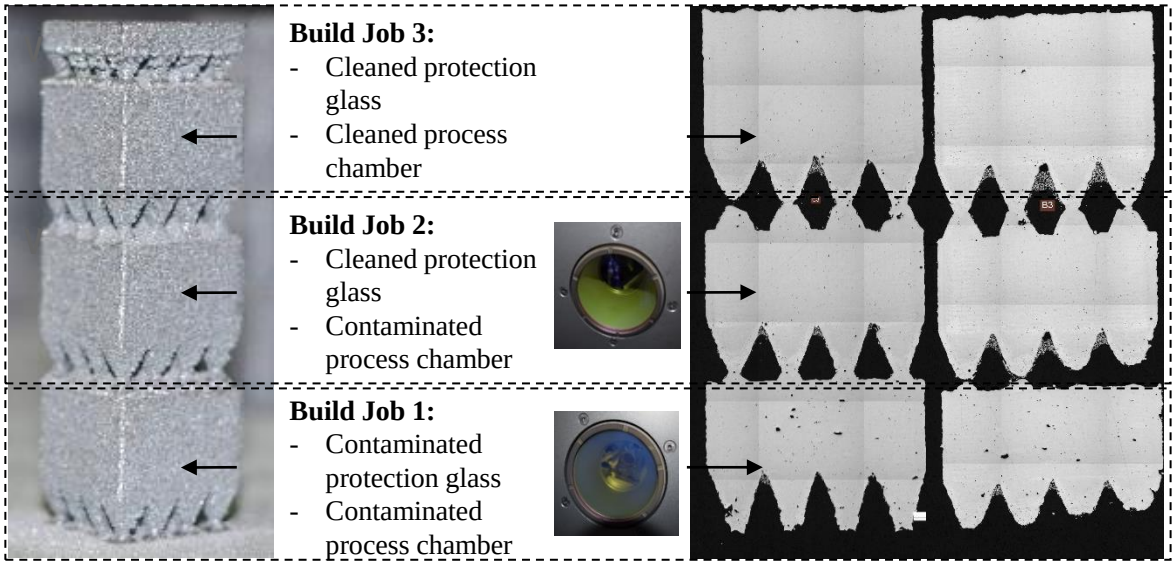

Figure 10 Influence of the weld fume contaminated protection glas on the part quality

It can be identified that the amount of porosity decreases drastically after the cleaning of the protection glass. Almost no weld spatter induced porosity > 50 µm occurs after removing the influence of a contaminated PG. Cleaning the build chamber does not seem to have a high influence of the remaining smaller porosity. To identify the influence of the contaminated PG on the porosity, its effect on the Laser Beam has to be analyzed. To this purpose the laser beam caustic gets measured before (cf. figure 11, clean PG = green caustic) and after the process (contaminated PG = brown caustic) for both lasers in machine 1.

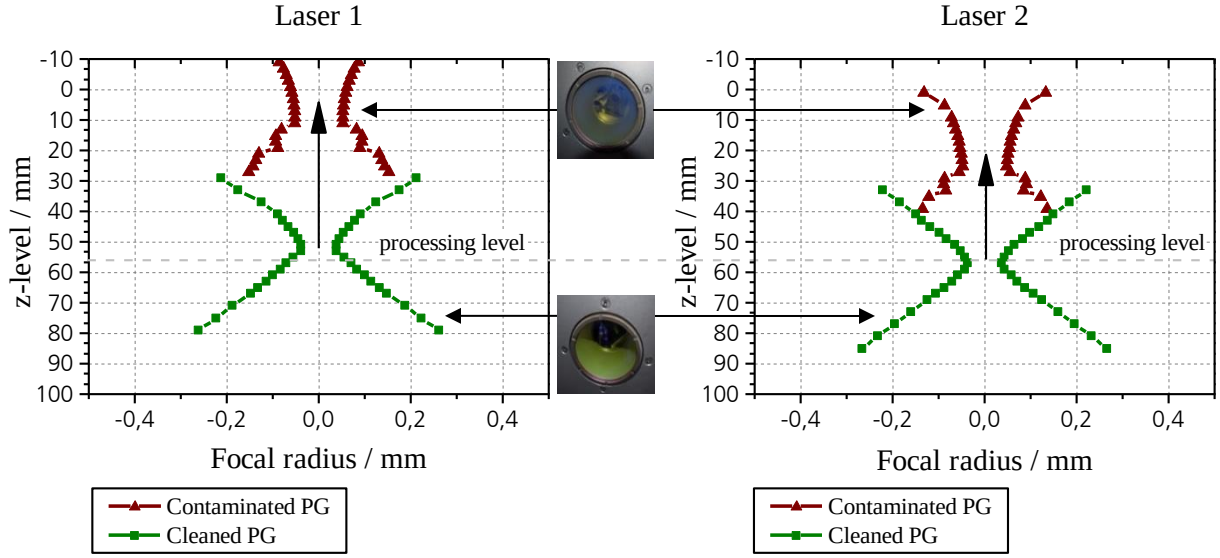

Figure 11 Influence of the weld fume contaminated protection glas on the laser focal level

What can be seen is the shift of the laser focus in dependence of the state of the protection glass for both lasers. If it is contaminated, the focus shifts in z-direction several millimeters. The laser power hardly does not get affected by the contaminated protection glass. A maximum

deviation of approx. 5 W could be measured. The absolute measured value of focus shift does not describe the value of it during the process. While measuring the caustic, the laser power is turned on at 650 W and the beam heats the protection glass for around 30 minutes in the exact same spot. This does not happen during the process where the laser beam moves constantly. Therefore the value of the focus shift during the process will not have the quantity of the one shown in figure 11. The focus shift leads to a decreasing intensity of the laser beam at the processing level. Thus the energy is distributed over a bigger area and not enough to fully melt existing weld spatters. This leads to the creation of weld spatter induced porosity and the increase of it over the build time.

Measures for process monitoring

The occurrence and amount of weld spatter induced porosity varies and is stochastically distributed. To have the ability to monitor these anomalies in the powder bed during the process, a Laser Line Scanner is implemented in the machine. This scanner measures a line in its height via optical triangulation. Moving the sensor translational over the powder bed via linear axes and stacking the lines digitally together, the topography of the powder bed can be measured with a resolution of roundabout 10 µm in z-direction. State of the art are so far image analysis of high resolution camera systems to analyze the quality of the powder layer. (cf. [11]).
Zenzinger, 2014 [19] showed the possibility of process monitoring via a CMOS camera system. A topographical measurement of the work plane via stripe light projection was introduced by *Zhang, 2016* (cf. [11]). Further in situ process monitoring of beam melting processes is listed and explained in *Grasso, 2017* [20] and *Everton, 2016* [21]. In figure 12 the comparison between the recording of the Laser Line Scanner system and a camera picture is shown.

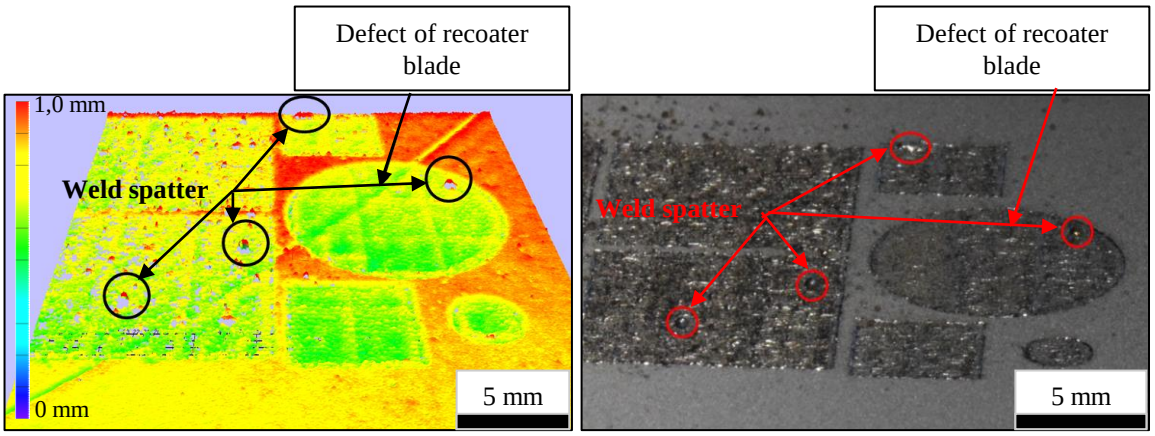

Figure 12 Recorded topography of a laser melted powder bed via a Laser Line Scanner in comparison with a camera picture (machine 2)

It can be shown that process characteristics can be identified throughout the topographical measurement of the fused area and the surrounding powder bed. The overlap of the single scan vectors can be seen as well as elevations that indicate weld spatters. In comparison with the camera pictures, those elevations can be determined as weld spatters. Machine 1 recoats the powder bed through a rotational movement of the recoating system. The line-wise deepening in the powder bed indicates a defect of the re-coater blade and can be identified on the already fused area. Such characteristics are hardly recognizable on the camera picture and cannot be quantified in form of

their height. In machine 1, the full monitoring of the powder bed via the Laser Line Scanner works automatically. It measures each layer after the Laser exposure and after the recoating process. Thus every part in every layer can be monitored. Figure 13 shows this for the cuboid produced. Also, in this instance, elevation and irregularities in the powder bed before and after the recoating can be identified.

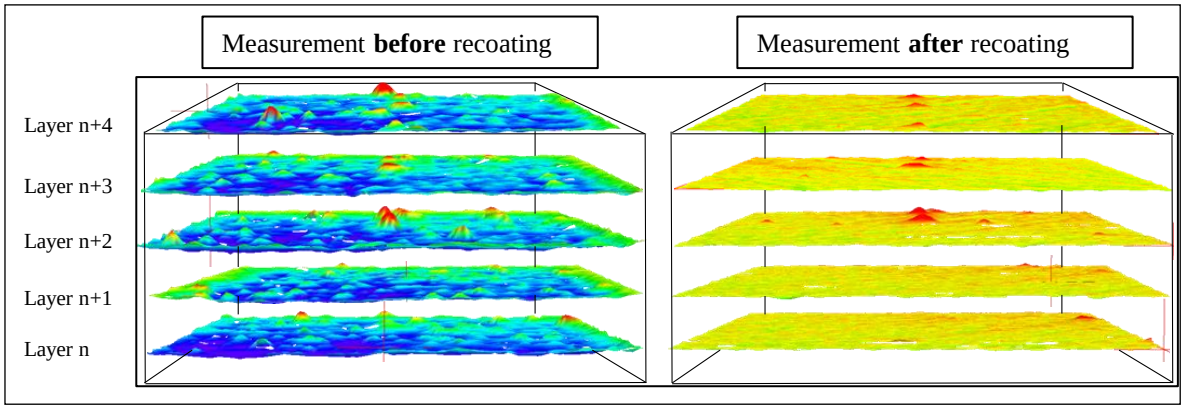

Figure 13 Principle of the automated measurement with the Laser Line Scanner system to analyze layerwise the part quality

To correlate between the recordings of the Laser Line Scanner and the porosity in the produced part, the part gets measured in each layer throughout the Laser Line Scanner and gets analyzed after the process via computer tomography automatically. With this method, pores can be measured in a spatially resolved way. A comparison between the Laser Line Scanner recordings and a CT-scan are shown in figure 14.

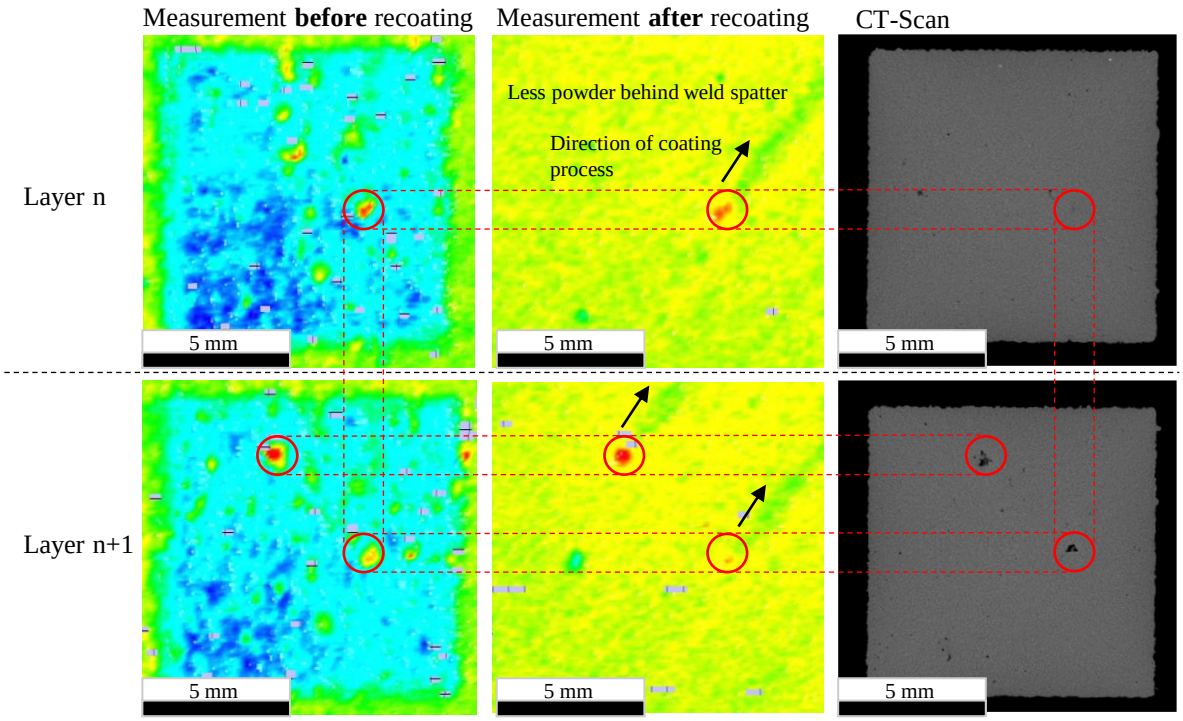

Figure 14 Correlation between with the Laser Line Scanner identified weld spatters and pores in the final part (machine 2)

It can be seen that on every spot where an elevation can be identified in the powder bed after the recoating process a pore also exists in the manufactured part. With this it can be explicitly proven that a monitoring of weld spatter induced porosity is possible with a Laser Line Scanner System.

Summary and future prospects

Within the scope of the performed investigation, a series production of specimen was simulated in the process of selective Laser Beam Melting. For this purpose two machines with two materials (AlSi10Mg, X3NiCoMoTi18-9-5) were used and for each machine, six build jobs in three different packing densities were produced. For each build job, the quasi static mechanical properties and the relative part densities were analyzed. The relative part densities were investigated for each build job on nine equally distributed specimens in two elevation levels. It can be seen, that the mechanical properties and rel. part densities decrease in the mean value and start to vary stronger for increasing packing densities on both machines. The reduction of the rel. part density is mainly caused by pores bigger than 50 µm and an edgy pore form. The reason for these pores are weld spatters who get welded in the part during the process. These particles show a diameter ten times bigger then the d90 value of the powder particle size distribution (60 µm). The introduced energy of the laser is not sufficient to fully melt these particles and therefore shade the laser light from melting the powder below the weld spatter. This leads to the emergence of pores.

To have the ability to monitor this weld spatter induced porosity, a Laser Line Scanner system got implemented in the production machine. This sensor moves translational over the powder bed and measures the topography of it. With this method weld spatters can be identified in form of elevations in the powder bed. In a comparison of the recordings with CT scans it can be shown,

that on the exact same spots where an elevation is detected a pore also exists in the final part. This proves that a process monitoring of weld spatter induced porosity is possible and useful with a Laser Line Scanner.

Further investigations are needed to clarify the causes for the occurrence of weld spatters to understand the phenomena completely. Based on those, further process monitoring and process optimizing methods can be derived. This leads to increasing part qualities and a higher reproducibility of the selective Laser Beam Melting process.

References

[1] R. Klose, “Industrie 4.0 und Additive Manufacturing,” https://www.empa.ch/web/s604/wef-industry-4.0?inheritRedirect=true.

[2] A. Müller, *EY‘sGlobal 3D printingReport 2016*, 2016.

[3] Hillebrecht Dr. Martin, “EDAG Insights 1/14 Generative Fertigung: EDAG Genesis,” http://www.edag.de/fileadmin/edag/downloads_files/INSIGHTS/EDAG_Insights_genesis_0114_d.pdf.

[4] Wohlers Associates, *Wohlers report 2016*: *3D printing and additive manufacturing state of the industry : annual worldwide progress report*, Wohlers Associates, Fort Collins (Colo.), 2016.

[5] “25 years of 3D printing at the BMW Group: Pioneers in additive manufacturing methods,” BMW Group Press Club, 11/18/2015, https://www.press.bmwgroup.com/global/article/detail/T0243462EN/25-years-of-3d-printing-at-the-bmw-group:-pioneers-in-additive-manufacturing-methods?language=en.

[6] “Series components made by 3D printers: BMW Group expands use of additive manufacturing processes,” BMW Group Press Club, 7/13/2016, https://www.press.bmwgroup.com/global/article/detail/T0261924EN/series-components-made-by-3d-printers:-bmw-group-expands-use-of-additive-manufacturing-processes?language=en.

[7] Erhard Brandl, “Additive manufactured AlSi10Mg samples using Selective Laser Melting (SLM):Microstructure, high cycle fatigue, and fracture behavior,” *Materials and Design,* 34 (2012), 2011.

[8] E. Wycisk, A. Solbach, S. Siddique et al., “Effects of Defects in Laser Additive Manufactured Ti-6Al-4V on Fatigue Properties,” *Physics Procedia*, vol. 56, pp. 371–378, 2014.

[9] Haijun Gong, “Influence of defects on mechanical properties of Ti–6Al–4 V componentsproduced by selective laser melting and electron beam melting,” *Materials and Design,* 86 (2015), 30.07.2015.

[10] D. F. S. Buchbinder, *Selective Laser Melting von Aluminiumgusslegierungen*, Shaker, Aachen, 2013.

[11] D. Zhang, *Entwicklung des Selective Laser Melting (SLM) für Aluminiumwerkstoffe*, Shaker, Aachen, 2004.

[12] A. Ladewig, G. Schlick, M. Fisser et al., “Influence of the shielding gas flow on the removal of process by-products in the selective laser melting process,” *Additive Manufacturing*, vol. 10, pp. 1–9, 2016.

[13] G. Repossini, V. Laguzza, M. Grasso et al., “On the use of spatter signature for in-situ monitoring of Laser Powder Bed Fusion,” *Additive Manufacturing*, vol. 16, pp. 35–48, 2017.

[14] Y. Liu, Y. Yang, S. Mai et al., “Investigation into spatter behavior during selective laser melting of AISI 316L stainless steel powder,” *Materials & Design*, vol. 87, pp. 797–806, 2015.

[15] J.-P. Weberpals, *Nutzen und Grenzen guter Fokussierbarkeit beim Laserschweißen*, Utz, München, 2010.

[16] T. Kühnle, K. Partes, and F. Vollertsen, eds., *Characterization of the thermal focus shift in a selective laser melting machine,*, 2012.

[17] I. Maskery, N. T. Aboulkhair, M. R. Corfield et al., “Quantification and characterisation of porosity in selectively laser melted Al? Si10?Mg using X-ray computed tomography,” *Materials Characterization*, vol. 111, pp. 193–204, 2016.
[18] M. Simonelli, C. Tuck, N. T. Aboulkhair et al., “A Study on the Laser Spatter and the Oxidation Reactions During Selective Laser Melting of 316L Stainless Steel, Al-Si10-Mg, and Ti-6Al-4V,” *Metallurgical and Materials Transactions A*, vol. 46, no. 9, pp. 3842–3851, 2015.
[19] G. Zenzinger, “Online-Prozesskontrolle bei der additiven Fertigung mittels Laserstrahlschmelzen,” *ZfP,* no. 140, pp. 51–54, 2014.
[20] M. Grasso and B. M. Colosimo, “Process defects and in situ monitoring methods in metal powder bed fusion: A review,” *Measurement Science and Technology*, vol. 28, no. 4, p. 44005, 2017.
[21] S. K. Everton, M. Hirsch, P. Stravroulakis et al., “Review of in-situ process monitoring and in-situ metrology for metal additive manufacturing,” *Materials & Design*, vol. 95, pp. 431–445, 2016.